Spectroscopy and high-power laser operation of monoclinic $Yb^{3+}:MgWO_4$ crystal

Pavel Loiko,[1,3] Mengting Chen,[1,4] Josep Maria Serres,[1] Magdalena Aguiló,[1] Francesc Díaz,[1] Haifeng Lin,[2] Ge Zhang,[2] Lizhen Zhang,[2] Zhoubin Lin,[2] Patrice Camy,[3] Shi-Bo Dai,[4] Zhenqiang Chen,[4] Yongguang Zhao,[5] Li Wang,[5] Weidong Chen,[2,5,*] Uwe Griebner,[5] Valentin Petrov,[5] and Xavier Mateos,[1]

[1]*Física i Cristal·lografia de Materials i Nanomaterials (FiCMA-FiCNA)-EMaS, Dept. Química Física i Inòrganica, Universitat Rovira i Virgili (URV), Campus Sescelades, E-43007 Tarragona, Spain*

[2]*Key Laboratory of Optoelectronic Materials Chemistry and Physics, Fujian Institute of Research on the Structure of Matter, Chinese Academy of Sciences, Fuzhou, 350002 Fujian, China*

[3]*Centre de recherche sur les Ions, les Matériaux et la Photonique (CIMAP), UMR 6252 CEA-CNRS-ENSICAEN, Université de Caen, 6 Boulevard du Maréchal Juin, 14050 Caen Cedex 4, France*

[4]*Department of Optoelectronic Engineering, Jinan University, Guangzhou 510632, China*

[5]*Max Born Institute for Nonlinear Optics and Short Pulse Spectroscopy, Max-Born-Str. 2a, D-12489 Berlin, Germany*

**Corresponding author: chenweidong@fjirsm.ac.cn*

Received XX Month XXXX; revised XX Month, XXXX; accepted XX Month XXXX; posted XX Month XXXX (Doc. ID XXXXX); published XX Month XXXX

Monoclinic (wolframite-type) monotungstate crystals are promising for rare-earth-doping. We report polarized room- and low-temperature spectroscopy, and efficient high-power laser operation of such a $Yb^{3+}:MgWO_4$ crystal featuring high stimulated-emission cross-section (σ_{SE} = 6.2×10^{-20} cm^2 at 1056.7 nm for light polarization $E \parallel N_m$), large Stark splitting of the ground-state (765 cm^{-1}), large gain bandwidth (26.1 nm for $E \parallel N_g$) and strong Raman response (most intense mode at 916 cm^{-1}). A diode-pumped $Yb^{3+}:MgWO_4$ laser generated 18.2 W at ~1056 nm with a slope efficiency of ~89% and a linearly polarized laser output.

http://dx.doi.org/10.1364/OL.99.099999

Recently, monoclinic wolframite-type ((Fe,Mn)WO_4, sp. gr. $P2/c$) magnesium tungstate crystals, $MgWO_4$, have emerged as promising host materials for doping with rare-earth ions (RE^{3+}) [1-3]. They belong to the crystal family of monoclinic transition metal monotungstates $M^{2+}WO_4$ (where M = Mg, Zn, Mn, Fe, Ni, *etc.*) [4]. So far, $MgWO_4$ (a = 4.6889 Å, b = 5.6753 Å, c = 4.9289 Å, β = 90.726° [5]) crystals were mostly studied for scintillators and for doping with transition-metal ions, e.g., Cr^{3+} [5,6]. $MgWO_4$ exhibits good thermo-mechanical properties (high thermal conductivity <κ> of 8.7 W/(mK) [7] and low anisotropy of thermal expansion: α_a = 11.22, α_b = 8.09 and α_c = 8.77 [10^{-6} K^{-1}] [3]). These properties are superior compared to another well-known crystal family of monoclinic double tungstates, $KLn(WO_4)_2$ [8], for which <κ> ≈ 3.5 W/mK and the thermal expansion tensor shows a significant anisotropy [9]. Besides, RE^{3+}-doped $MgWO_4$ shows attractive spectroscopic properties (broad and intense emission bands for polarized light, large Stark splitting, high luminescence quantum yield and Raman activity) [1-3]. These advantages originate from the low-symmetry structure and the substantial difference in ionic radii of the RE^{3+} dopants and the host-forming Mg^{2+} cations [10].

Regarding laser operation of RE^{3+}-doped $MgWO_4$ crystals, previous studies focused mostly on the spectral range of ~2 μm using thulium (Tm^{3+}) [2, 10-12] and holmium (Ho^{3+}) [3] ion doping. A diode-pumped continuous-wave (CW) $Tm^{3+}:MgWO_4$ laser generated 3.09 W at 2022-2034 nm with a slope efficiency η of 50% [11]. A graphene mode-locked (ML) $Tm^{3+}:MgWO_4$ laser delivered 86 fs pulses at 2017 nm featuring a bandwidth of 53 nm at a repetition rate of 76 MHz [12].

For laser emission at ~1 μm, ytterbium (Yb^{3+}) ion doping holds a huge potential. This is because Yb^{3+} has a simple energy-level scheme eliminating the unwanted energy-transfer processes and leading to high Stokes pump efficiency and weak heat loading [13]. The larger Stark splitting of the ground-state ($^2F_{7/2}$) (as compared to Nd^{3+}) is a prerequisite for broader emission at ~1 μm. So far, the growth and preliminary spectroscopy of $Yb^{3+}:MgWO_4$ crystal were reported [1,14]. A semiconductor saturable absorber mirror

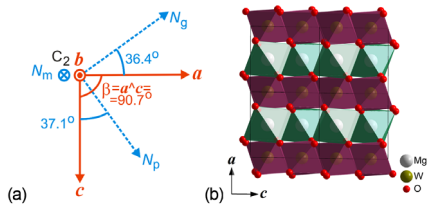

Fig. 1. (a) Orientation of the optical indicatrix axes (N_p, N_m and N_g) in monoclinic Yb:$MgWO_4$ crystal: ***a***, ***b*** and ***c*** – crystallographic axes, C_2 – 2-fold symmetry axis; (b) crystal structure in projection to the ***a*-*c*** plane.

(SESAM) ML Yb^{3+}:$MgWO_4$ laser delivered 125 fs pulses at 1065 nm at a repetition rate of 117 MHz [15].

In this work, we report a detailed room- and low-temperature polarization-resolved spectroscopy of Yb^{3+}:$MgWO_4$ paving the way towards its highly-efficient and high-power diode-pumped laser operation. We consider this work as a first step towards high-power mode-locked bulk and thin-disk lasers based on Yb^{3+}:$MgWO_4$.

The 1.25 at.% Yb^{3+}:$MgWO_4$ crystal was grown by the Top-Seeded Solution Growth (TSSG) method using Na_2WO_4 as a solvent [1,3]. Its structure (monoclinic, sp. gr. C^4_{2h} – $P2/c$) [16] was confirmed by using X-ray powder diffraction. In $MgWO_4$, the Yb^{3+} ions are replacing the Mg^{2+} ones in a single type of sites (Wyckoff position: 2*f*, site symmetry: C_2, VI-fold oxygen coordination in distorted [Mg|YbO_6] polyhedra), Fig. 1(b). Charge compensation is provided by Na^+ cations entering from the melt [3]. The corresponding ionic radii are R_{Yb} = 0.868 Å, R_{Mg} = 0.72 Å and R_{Na} = 1.02 Å. The concentration of Yb^{3+} ions in the crystal N_{Yb} was 1.82×10^{20} cm^{-3} (as determined by Inductively Coupled Plasma Atomic Emission Spectroscopy). Note that the increase of Yb^{3+} doping level is mainly limited by the heterovalent doping mechanism; this would also lead to the deteriorated thermal properties of the crystal.

Monoclinic Yb^{3+}:$MgWO_4$ is optically biaxial (point group 2/*m*). At the wavelength of ~1 μm, the principal refractive indices are n_p = 1.97, n_m = 2.03 and n_g = 2.13±0.02 according to the $n_p < n_m < n_g$ convention. One of the optical indicatrix axes (N_m) coincides with the C_2 symmetry axis (the ***b***-axis) and other two (N_p and N_g) are lying in the orthogonal mirror plane (the ***a*-*c*** plane), Fig. 1. The angle N_p^***c*** = 37.1°, measured within the obtuse angle β.

Room-temperature (RT, 293 K) absorption, σ_{abs}, cross-sections corresponding to the $^2F_{7/2} \rightarrow {}^2F_{5/2}$ transition are shown in Fig. 2(a) for the principal light polarizations ***E*** || N_p, N_m and N_g. The maximum σ_{abs} is 6.16×10^{-20} cm^2 at 974.0 nm (the zero-phonon line, ZPL, at RT) and the corresponding full width at half maximum (FWHM) of the absorption peak is 5.6 nm (for ***E*** || N_g). The stimulated-emission (SE) cross-sections, σ_{SE}, were calculated using a combination of the Füchtbauer-Ladenburg (F-L) equation [17] based on the measured luminescence spectra, and the reciprocity method (RM) [18] based on the determined Stark splitting). The maximum σ_{SE} reaches 6.2×10^{-20} cm^2 at 1056.7 nm for ***E*** || N_m. Yb^{3+}:$MgWO_4$ exhibits a strong anisotropy of the SE cross-sections at this wavelength: $\sigma_{SE}(m)$: $\sigma_{SE}(g)$ = 3.7 and $\sigma_{SE}(m)$: $\sigma_{SE}(p)$ = 5.5, which is a prerequisite for a linearly polarized laser emission. From the luminescence spectra (measured with λ_{exc} = 972 nm), the emission bandwidth is 18.7 nm (***E*** || N_m) and >50 nm (structured spectrum, ***E*** || N_g). Yb^{3+}:$MgWO_4$ exhibits a single-exponential luminescence decay with a lifetime τ_{lum} of 366 μs, as measured for a powdered sample to avoid radiation trapping. The $^2F_{5/2} \rightarrow {}^2F_{7/2}$ transition of Yb^{3+} represents a quasi-three-level laser scheme with reabsorption.

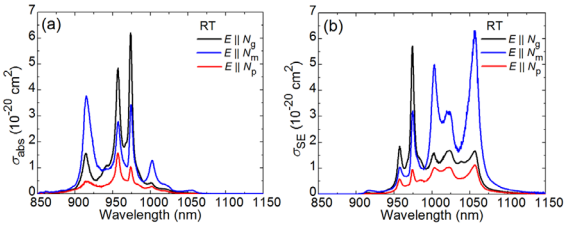

Fig. 2. RT (a) absorption, σ_{abs}, and (b) stimulated-emission, σ_{SE}, cross-section spectra of Yb^{3+} in monoclinic $MgWO_4$ for ***E*** || N_p, N_m and N_g.

Thus, gain cross-sections, $\sigma_{gain} = \beta\sigma_{SE} - (1-\beta)\sigma_{abs}$, where $\beta = N_2(^2F_{5/2})/N_{Yb}$ is the inversion ratio, and N_2 is the upper laser level population, are calculated to predict the spectral properties of laser emission, see Fig. 3 for ***E*** || N_m and ***E*** || N_g. For ***E*** || N_m, a local peak in the gain spectra is observed at ~1057 nm and the gain bandwidth $\Delta\lambda_g$ is 15.1 nm (FWHM, for β = 0.1). For ***E*** || N_g, a similar behavior is observed while the gain spectra are broader, $\Delta\lambda_g$ = 26.1 nm.

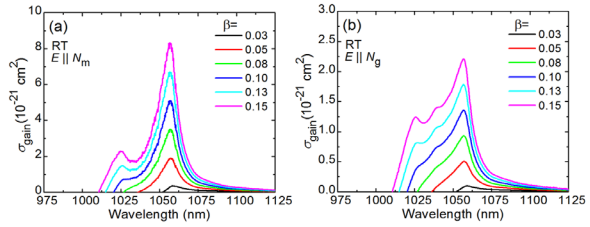

Fig. 3. RT gain cross-sections, $\sigma_{gain} = \beta\sigma_{SE} - (1-\beta)\sigma_{abs}$, where $\beta = N_2(^2F_{5/2})/N_{Yb}$ is the inversion ratio, for Yb^{3+} ions in monoclinic $MgWO_4$ crystal. The light polarizations are (a) ***E*** || N_m and (b) ***E*** || N_g.

The polarized Raman spectra of an N_m-cut Yb^{3+}:$MgWO_4$ crystal are shown in Fig. 4 for the $m(ij)m$, where $i, j = p, g$, configurations (using Porto's notation). The excitation wavelength is λ_{exc} = 514 nm. The most intense vibration is observed at 915.7 cm^{-1} (the FWHM of the Raman band is 15.0 cm^{-1}) and assigned to symmetric stretching W–O vibrations $\nu_1(A_{1g})$ in the WO_6 octahedra [2]. Yb^{3+}:$MgWO_4$ is promising for self-Raman frequency conversion.

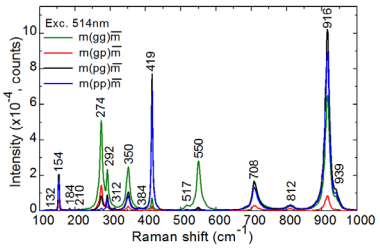

Fig. 4. Polarized Raman spectra for Yb^{3+}:$MgWO_4$ for the $m(xy)m$ configurations (Porto's notation), *numbers* indicate the Raman frequencies in cm^{-1}.

To resolve the Stark splitting of Yb^{3+} multiplets, the absorption and luminescence spectra were measured in the temperature range of 6–300 K, Fig. 5. For Yb^{3+} ions in C_2 symmetry sites, there is a total of 2*J* + 1 Stark sub-levels for each $^{2S+1}L_J$ multiplet, numbered as 0..3 for $^2F_{7/2}$ and 0'..2' for $^2F_{5/2}$. The interpretation of the Stark transitions was carried out accounting for the Raman spectra.

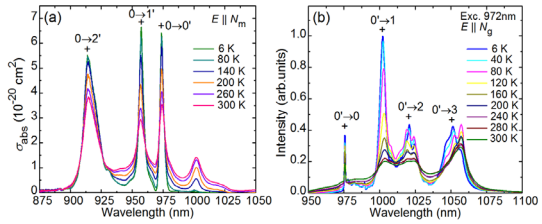

Fig. 5. Low temperature spectroscopy of Yb:$MgWO_4$: (a) absorption spectra for $\boldsymbol{E} \parallel N_m$; (b) luminescence spectra for $\boldsymbol{E} \parallel N_g$, λ_{exc} = 972 nm. The "+" marks indicate Stark transitions.

The energy-level scheme of Yb^{3+} ions in $MgWO_4$ is shown in Fig. 6(a). The ZPL (the transition between the lowest sub-levels of both multiplets) has an energy E_{ZPL} = 10275 cm^{-1}. The partition functions for the lower and upper multiplets are Z_1 = 1.352 and Z_2 = 1.469, respectively (Z_1/Z_2 = 0.920). The total Stark splitting of the ground-state, $\Delta E(^2F_{7/2})$ = 765 cm^{-1}, exceeds that in other known tungstate crystals [8,19], Fig. 6(b). For the RE^{3+} ions, the barycenter of any $^{2S+1}L_J$ $4f^n$ multiplet shows a linear variation vs. the barycenter of any other isolated multiplet, which is expressed as a barycenter plot [20], see Fig. 6(c). The barycenter energies $<E(^2F_{5/2})>$ and $<E(^2F_{7/2})>$ for Yb^{3+}:$MgWO_4$ agree well with this plot.

In Table 1, we compare the emission properties of Yb^{3+}:$MgWO_4$ with other well-known tungstate laser crystals, namely, monoclinic (sp. gr. $C2/c$) Yb^{3+}:$KLu(WO_4)_2$ [8] and tetragonal disordered (sp. gr. $I4_1/a$) Yb^{3+}:$NaY(WO_4)_2$ [21]. Yb^{3+}:$MgWO_4$ has higher SE cross-sections, while its gain bandwidths are comparable to those of monoclinic double tungstates.

Table 1. Spectroscopic Properties* of Yb^{3+} in Tungstate Crystals

Crystal	Site	λ_{em}, nm	$\Delta\lambda_g$, nm	σ_{SE}, $10^{-20}cm^2$	τ_{lum}, μs	Ref.
$NaY(WO_4)_2$	S_4	1018(π)	33.9(π)	1.38(π)	309	[21]
		1024(σ)	25.9(σ)	0.86(σ)		
$KLu(WO_4)_2$	C_2	1026.7(*m*)	20.2(*m*)	2.6(*m*)	275	[8]
		1041.2(*p*)	28.0(*p*)	1.3(*p*)		
$MgWO_4$	C_2	1056.7(*m*)	15.1(*m*)	6.25(*m*)	366	*
		1056.6(*g*)	26.1(*g*)	1.68(*g*)		

*λ_{em} – emission wavelength, $\Delta\lambda_g$ – gain bandwidth (β = 0.1), σ_{SE} – SE cross-section, τ_{lum} – reabsorption-free luminescence lifetime.

For laser experiments, a rectangular sample was cut from the 1.25 at.% Yb^{3+}:$MgWO_4$ crystal for light propagation along the N_p optical indicatrix axis (N_p-cut). It had a thickness of 3.1 mm and an aperture of 4×4 mm^2. This crystal orientation was selected because it gives access to the high-gain light polarization ($\boldsymbol{E} \parallel N_m$). The uncoated crystal was mounted in a Cu-holder using Indium foil for better thermal thermal contact from all lateral sides. The holder was cooled to ~14 °C by circulating water. The crystal was inserted in a compact plano-plano (microchip-type) laser cavity, Fig. 7, formed by a flat pump mirror (PM) coated for high transmission (HT) at 0.88-0.99 μm and for high reflection (HR) at 1.02-1.23 μm, and a set of flat output couplers (OCs) with a transmission T_{OC} of 0.5%...10% at the laser wavelength. Both the PM and the OC were placed close to the crystal with minimum air gaps, so that the geometrical cavity length was ~3.1 mm. The microchip laser concept benefits from a robust and compact design and good cavity stability.

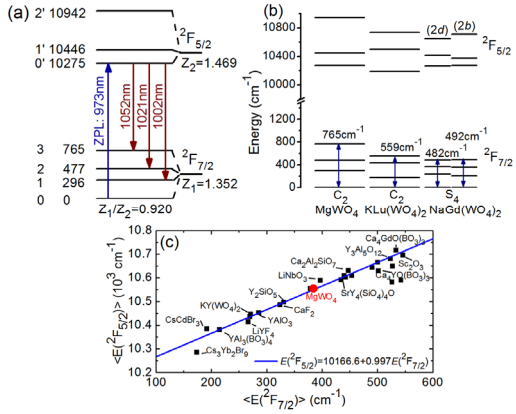

Fig. 6. Stark splitting of Yb^{3+} multiplets in $MgWO_4$: (a) Energy-level scheme, *numbers* indicate the energy in cm^{-1}, $Z_{1(2)}$ are the partition functions; (b) Stark splitting of Yb^{3+} in tungstate crystals: $MgWO_4$, $KLu(WO_4)_2$ [8], $NaGd(WO_4)_2$ [19] (C_2 and S_4 – Yb^{3+} site symmetries); (c) barycenter plot [20] for Yb^{3+} ions showing the result for $MgWO_4$.

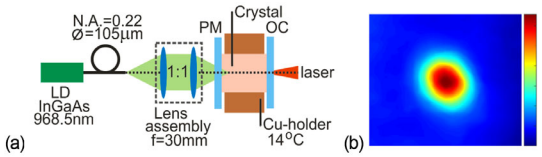

Fig. 7. (a) Scheme of the compact diode-pumped Yb^{3+}:$MgWO_4$ laser: LD – laser diode, PM – pump mirror, OC – output coupler; (b) typical profile of the laser beam in the far-field (the beam ellipticity originates from the astigmatic thermal lens), $P_{abs} \approx 10$ W.

The N_p-cut Yb^{3+}:$MgWO_4$ crystal generated a maximum output power of 18.2 W at ~1056 nm with a slope efficiency η of ~89% (*vs.* the absorbed pump power P_{abs}), Fig. 8(a). The laser threshold was at P_{abs} = 0.54 W and the optical-to-optical efficiency η_{opt} amounted to 33.7% (*vs.* the pump power incident on the crystal). All these values are specified for T_{OC} = 10%. The laser output was linearly polarized ($\boldsymbol{E} \parallel N_m$) and the polarization was intrinsically selected by the gain anisotropy, Fig. 2(b). For all studied OCs, the emission wavelength was ~1.06 μm, Fig. 3(a), in agreement with the gain spectra. A slight blue-shift of the laser wavelength with increasing output coupling was detected, Fig. 8(b), and ascribed to the quasi-three-level nature of the Yb^{3+} laser scheme exhibiting reabsorption at the laser wavelength. The laser operation in the plano-plano cavity was supported by a positive (focusing) thermal lens. For T_{OC} < 10%, power scaling was limited by a thermal roll-over probably because of too high intracavity laser intensity. The determined laser slope efficiency gives an estimation of the roundtrip passive loss L of 0.35% (loss coefficient: δ_{loss} = 0.0056 cm^{-1}). No crystal fracture was observed up to at least P_{abs} = 22.5 W (limited by the available pump).

In Table 2, we compare the output characteristics of compact diode-pumped lasers based on Yb^{3+}-doped oxide crystals and reported recently. The superior laser results achieved with Yb^{3+}:$MgWO_4$ compared to previous studies with other tungstate crystals, Yb^{3+}:$NaY(WO_4)_2$ and Yb^{3+}:$KLu(WO_4)_2$, are attributed to its better thermo-mechanical properties. crystals, Yb^{3+}:$NaY(WO_4)_2$ and Yb^{3+}:$KLu(WO_4)_2$, are attributed to its better thermo-mechanical properties.

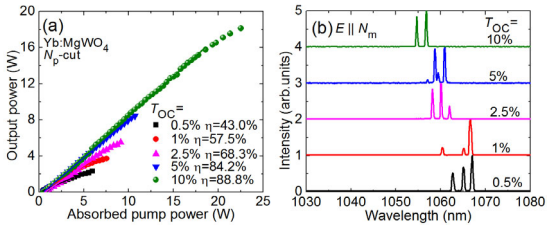

Fig. 8. Diode-pumped compact Yb^{3+}:$MgWO_4$ laser: (a) input-output dependences, η – slope efficiency; (b) typical laser emission spectra. The crystal orientation is N_p-cut, the laser polarization is $\boldsymbol{E} \parallel N_m$.

Table 2. Output Characteristics* of Compact Diode-Pumped Ytterbium Lasers Based on Oxide Crystals Reported So Far

Crystal	Yb, at.%	P_{out}, W	λ_L, nm	P_{th}, W	η, %	Ref.
$Yb:LuVO_4$	1.5	8.3	1031	2.6	80	[22]
$Yb:CaGdAlO_4$	8	7.79	~1061	2.0	**84**	[13]
$Yb:LuAlO_3$	2	9.6	1041	~1.5	74	[23]
$Yb:NaY(WO_4)_2$	4.8	5.2	1045	1.20	50	[24]
$Yb:KLu(WO_4)_2$	5.2	11.0	~1045	0.61	80	[25]
$Yb:MgWO_4$	1.25	**18.2**	~1056	0.54	**89**	**
$Yb:Ca_4GdO(BO_3)_3$	10	**18.2**	1032	~1	70	[26]
$Yb:YAl_3(BO_3)_4$	5.6	10.6	1042	0.79	72	[27]
$Yb:Lu_3Ga_5O_{12}$	7.1	8.97	1040	1.22	75	[28]

*P_{out} – output power, λ_L – laser wavelength; P_{th} – threshold pump power, η – slope efficiency (*vs.* absorbed pump power); **This work.

To conclude, monoclinic Yb^{3+}:$MgWO_4$ is a promising crystal for compact, highly-efficient and high-power lasers at ~1 μm thanks to a combination of attractive thermal and spectroscopic properties. We report on the first laser operation of Yb^{3+}:$MgWO_4$ in a microchip-type laser cavity yielding >18 W of linearly polarized output at ~1.06 μm with a slope efficiency (88.8%) almost approaching the Stokes limit, $\eta_{St} = \lambda_P/\lambda_L = 91.7\%$. This is attributed to weak non-radiative relaxation, low optical losses and good mode-matching provided by the positive thermal lens for the selected crystal orientation and the results achieved in this work represent a record for Yb^{3+}-doped tungstate laser crystals.

Funding. National Natural Science Foundation of China (61975208, 51761135115, 61850410533, 61575199, 61875199); Deutsche Forschungsgemeinschaft (PE 607/14-1); Laserlab-Europe (654148); Natural Science Foundation of Jiangsu Province (SBK2019030177); Sino-German Scientist Cooperation and Exchanges Mobility Programme (M-0040); Spanish Government, MINECO (MAT2016-75716-C2-1-R (AEI/FEDER,UE); Generalitat de Catalunya (2017SGR755).

Acknowledgment. Yongguang Zhao acknowledges financial support from the Alexander von Humboldt Foundation through a Humboldt fellowship.

Disclosures. The authors declare no conflicts of interest.

References

1. L. Zhang, W. Chen, J. Lu, H. Lin, L. Li, G. Wang, G. Zhang, and Z. Lin, Opt. Mater. Express **6**, 1627 (2016).
2. L. Zhang, H. Lin, G. Zhang, X. Mateos, J. M. Serres, M. Aguiló, F. Díaz, U. Griebner, V. Petrov, Y. Wang, P. Loiko, E. Vilejshikova, K. Yumashev, Z. Lin, and W. Chen, Opt. Express **25**, 3682 (2017).
3. L. Zhang, P. Loiko, J.M. Serres, E. Kifle, H. Lin, G. Zhang, E. Vilejshikova, E. Dunina, A. Kornienko, L. Fomicheva, U. Griebner, V. Petrov, Z. Lin, W. Chen, K. Subbotin, M. Aguiló, F. Díaz, and X. Mateos, J. Lumin. **213**, 316 (2019).
4. E. Cavalli, A. Belletti, and M. G. Brik, J. Phys. Chem. Solids **69**, 29 (2008).
5. V. B. Mikhailik, H. Kraus, V. Kapustyanyk, M. Panasyuk, P. Yu, V. Tsybulskyi, and L. Vasylechko, J. Phys.: Cond. Matter **20**, 365219 (2008).
6. L. Li, Y. Yu, G. Wang, L. Zhang, and Z. Lin, Cryst. Eng. Comm. **15**, 6083 (2013).
7. L. Zhang, Y. Huang, S. Sun, F. Yuan, Z. Lin, and G. Wang, J. Lumin. **169,** 161 (2016).
8. V. Petrov, M. C. Pujol, X. Mateos, Ò. Silvestre, S. Rivier, M. Aguiló, R. M. Solé, J. H. Liu, U. Griebner, and F. Díaz, Laser Photon. Rev. **1**, 179 (2007).
9. P. A. Loiko, K. V. Yumashev, N. V. Kuleshov, G. E. Rachkovskaya, and A. A. Pavlyuk, Opt. Mater. **34**, 23 (2011).
10. P. Loiko, L. Zhang, J. M. Serres, Y. Wang, M. Aguiló, F. Díaz, Z. Lin, H. Lin, G. Zhang, E. Vilejshikova, E. Dunina, A. Kornienko, L. Fomicheva, V. Petrov, U. Griebner, W. Chen, and X. Mateos, J. Alloys Compd. **763**, 581 (2018).
11. P. Loiko, J. M. Serres, X. Mateos, M. Aguiló, F. Díaz, L. Zhang, Z. Lin, H. Lin, G. Zhang, K. Yumashev, V. Petrov, U. Griebner, Y. Wang, S. Y. Choi, F. Rotermund, and W. Chen, Opt. Lett. **42**, 1177 (2017).
12. Y. Wang, W. Chen, M. Mero, L. Zhang, H. Lin, Z. Lin, G. Zhang, F. Rotermund, Y. J. Cho, P. Loiko, X. Mateos, U. Griebner, and V. Petrov, Opt. Lett. **42**, 3076 (2017).
13. P. Loiko, J. M. Serres, X. Mateos, X. Xu, J. Xu, V. Jambunathan, A. Lucianetti, T. Mocek, X. Zhang, U. Griebner, V. Petrov, M. Aguiló, F. Díaz, and A. Major, Opt. Lett. **42**, 2431 (2017).
14. J. Lu, H. Lin, G. Zhang, B. Li, L. Zhang, Z. Lin, Y.-F. Chen, V. Petrov, and W. Chen, Laser Phys. Lett. **14**, 085807 (2017)
15. H. Lin, G. Zhang, L. Zhang, Z. Lin, F. Pirzio, A. Agnesi, V. Petrov, and W. Chen, Opt. Express **25**, 11827 (2017).
16. V. B. Kravchenko, J. Struct. Chem. **10**, 139 (1969).
17. B. Aull and H. Jenssen, IEEE J. Quantum Electron. **18**, 925 (1982).
18. S. A. Payne, L. L. Chase, L. K. Smith, W. L. Kway, and W. F. Krupke, IEEE J. Quantum Electron. **28**, 2619 (1992).
19. C. Cascales, M. D. Serrano, F. Esteban-Betegón, C. Zaldo, R. Peters, K. Petermann, G. Huber, L. Ackermann, D. Rytz, C. Dupré, M. Rico J. Liu, U. Griebner, and V. Petrov, Phys. Rev. B **74**, 174114 (2006).
20. P. H. Haumesser, R. Gaumé, B. Viana, E. Antic-Fidancev, and D. Vivien, J. Phys.: Cond. Matter **13**, 5427 (2001).
21. A. Garcia-Cortes, J. M. Cano-Torres, M. D. Serrano, C. Cascales, C. Zaldo, S. Rivier, X. Mateos, U. Griebner, and V. Petrov, IEEE J. Quantum Electron. **43**, 758 (2007).
22. J. Liu, V. Petrov, H. Zhang, J. Wang, and M. Jiang, Opt. Lett. **31**, 3294 (2006).
23. A. Rudenkov, V. Kisel, A. Yasukevich, K. Hovhannesyan, A. Petrosyan, and N. Kuleshov, Opt. Lett. **42**, 2415 (2017).
24. J. Liu, H. Zhang, J. Wang, and V. Petrov, Opt. Express **15**, 12900 (2007).
25. J. Liu, V. Petrov, X. Mateos, H. Zhang, and J. Wang, Opt. Lett. **32**, 2016 (2007).
26. X. Chen, L. Wang, J. Liu, Y. Guo, W. Han, H. Xu, H. Yu, and H. Zhang, Opt. Laser Tehcnol. **79**, 74 (2016).
27. J. Liu, X. Mateos, H. Zhang, J. Li, J. Wang, and V. Petrov, IEEE J. Quantum Electron. **43**, 385 (2007).
28. J. M. Serres, V. Jambunathan, P. Loiko, X. Mateos, H. Yu, H. Zhang, J. Liu, A. Lucianetti, T. Mocek, K. Yumashev, U. Griebner, V. Petrov, M. Aguiló, and F. Díaz, Opt. Mater. Express **6**, 46 (2016).

References

1. L. Zhang, W. Chen, J. Lu, H. Lin, L. Li, G. Wang, G. Zhang, and Z. Lin, "Characterization of growth, optical properties, and laser performance of monoclinic Yb:$MgWO_4$ crystal," Opt. Mater. Express **6**(5), 1627-1634 (2016).
2. L. Zhang, H. Lin, G. Zhang, X. Mateos, J. M. Serres, M. Aguiló, F. Díaz, U. Griebner, V. Petrov, Y. Wang, P. Loiko, E. Vilejshikova, K. Yumashev, Z. Lin, and W. Chen, "Crystal growth, optical spectroscopy and laser action of Tm^{3+}-doped monoclinic magnesium tungstate," Opt. Express **25**(4), 3682-3693 (2017).
3. L. Zhang, P. Loiko, J.M. Serres, E. Kifle, H. Lin, G. Zhang, E. Vilejshikova, E. Dunina, A. Kornienko, L. Fomicheva, U. Griebner, V. Petrov, Z. Lin, W. Chen, K. Subbotin, M. Aguiló, F. Díaz, and X. Mateos, "Growth, spectroscopy and first laser operation of monoclinic Ho^{3+}:$MgWO_4$ crystal," J. Lumin. **213**, 316-325 (2019).
4. E. Cavalli, A. Belletti, and M. G. Brik, "Optical spectra and energy levels of the Cr^{3+} ions in MWO_4 (M = Mg, Zn, Cd) and $MgMoO_4$ crystals," J. Phys. Chem. Solids **69**(1), 29-34 (2008).
5. V. B. Mikhailik, H. Kraus, V. Kapustyanyk, M. Panasyuk, P. Yu, V. Tsybulskyi, and L. Vasylechko, "Structure, luminescence and scintillation properties of the $MgWO_4$–$MgMoO_4$ system," J. Phys.: Cond. Matter **20**(36), 365219-1–8 (2008).
6. L. Li, Y. Yu, G. Wang, L. Zhang, and Z. Lin, "Crystal growth, spectral properties and crystal field analysis of Cr^{3+}:$MgWO_4$," Cryst. Eng. Comm. **15**(30), 6083-6089 (2013).
7. L. Zhang, Y. Huang, S. Sun, F. Yuan, Z. Lin, and G. Wang, "Thermal and spectral characterization of Cr^{3+}:$MgWO_4$ – a promising tunable laser material," J. Lumin. **169,** Part A, 161-164 (2016).
8. V. Petrov, M. C. Pujol, X. Mateos, Ò. Silvestre, S. Rivier, M. Aguiló, R. M. Solé, J. H. Liu, U. Griebner, and F. Díaz, "Growth and properties of $KLu(WO_4)_2$, and novel ytterbium and thulium lasers based on this monoclinic crystalline host," Laser Photon. Rev. **1**(2), 179-212 (2007).
9. P.A. Loiko, K.V. Yumashev, N.V. Kuleshov, G.E. Rachkovskaya, and A.A. Pavlyuk, "Detailed characterization of thermal expansion tensor in monoclinic $KRe(WO_4)_2$ (where Re = Gd, Y, Lu, Yb)," Opt. Mater. **34**(1), 23-26 (2011).
10. P. Loiko, L. Zhang, J.M. Serres, Y. Wang, M. Aguiló, F. Díaz, Z. Lin, H. Lin, G. Zhang, E. Vilejshikova, E. Dunina, A. Kornienko, L. Fomicheva, V. Petrov, U. Griebner, W. Chen, and X. Mateos, "Monoclinic Tm:$MgWO_4$ crystal: Crystal-field analysis, tunable and vibronic laser demonstration," J. Alloys Compd. **763**, 581-591 (2018).
11. P. Loiko, J. M. Serres, X. Mateos, M. Aguiló, F. Díaz, L. Zhang, Z. Lin, H. Lin, G. Zhang, K. Yumashev, V. Petrov, U. Griebner, Y. Wang, S. Y. Choi, F. Rotermund, and W. Chen, "Monoclinic Tm^{3+}:$MgWO_4$: a promising crystal for continuous-wave and passively Q-switched lasers at ~2 μm," Opt. Lett. **42**(6), 1177-1180 (2017).
12. Y. Wang, W. Chen, M. Mero, L. Zhang, H. Lin, Z. Lin, G. Zhang, F. Rotermund, Y. J. Cho, P. Loiko, X. Mateos, U. Griebner, and V. Petrov, "Sub-100 fs Tm:$MgWO_4$ laser at 2017 nm mode locked by a graphene saturable absorber," Opt. Lett. **42**(16), 3076-3079 (2017).
13. P. Loiko, J. M. Serres, X. Mateos, X. Xu, J. Xu, V. Jambunathan, A. Lucianetti, T. Mocek, X. Zhang, U. Griebner, V. Petrov, M. Aguiló, F. Díaz, and A. Major, "Microchip Yb:$CaLnAlO_4$ lasers up to 91% slope efficiency," Opt. Lett. **42**(13), 2431-2434 (2017).
14. J. Lu, H. Lin, G. Zhang, B. Li, L. Zhang, Z. Lin, Y.-F. Chen, V. Petrov, and W. Chen, "Direct generation of an optical vortex beam from a diode-pumped Yb:$MgWO_4$ laser," Laser Phys. Lett. **14**(8), 085807-1-6 (2017)
15. H. Lin, G. Zhang, L. Zhang, Z. Lin, F. Pirzio, A. Agnesi, V. Petrov, and W. Chen, "Continuous-wave and SESAM mode-locked femtosecond operation of a Yb:$MgWO_4$ laser," Opt. Express **25**(10), 11827-11832 (2017).
16. V. B. Kravchenko, "Crystal structure of the monoclinic form of magnesium tungstate $MgWO_4$," J. Struct. Chem. **10**(1), 139-140 (1969).
17. B. Aull and H. Jenssen, "Vibronic interactions in Nd:YAG resulting in nonreciprocity of absorption and stimulated emission cross sections," IEEE J. Quantum Electron. **18**(5), 925-930 (1982).
18. S. A. Payne, L. L. Chase, L. K. Smith, W. L. Kway, and W. F. Krupke, "Infrared cross-section measurements for crystals doped with Er^{3+}, Tm^{3+}, and Ho^{3+}," IEEE J. Quantum Electron. **28**(11), 2619-2630 (1992).
19. C. Cascales, M. D. Serrano, F. Esteban-Betegón, C. Zaldo, R. Peters, K. Petermann, G. Huber, L. Ackermann, D. Rytz, C. Dupré, and M. Rico, "Structural, spectroscopic, and tunable laser properties of Yb^{3+}-doped $NaGd(WO_4)_2$," Phys. Rev. B **74**(17), 174114-1-15 (2006).
20. P. H. Haumesser, R. Gaumé, B. Viana, E. Antic-Fidancev, and D. Vivien, "Spectroscopic and crystal-field analysis of new Yb-doped laser materials," J. Phys.: Cond. Matter **13**(23), 5427 (2001).
21. A. Garcia-Cortes, J. M. Cano-Torres, M. D. Serrano, C. Cascales, C. Zaldo, S. Rivier, X. Mateos, U. Griebner, and V. Petrov, "Spectroscopy and lasing of Yb-doped $NaY(WO_4)_2$: tunable and femtosecond mode-locked laser operation," IEEE J. Quantum Electron. **43**(9), 758-764 (2007).
22. J. Liu, V. Petrov, H. Zhang, J. Wang, and M. Jiang, "High-power laser performance of *a*-cut and *c*-cut Yb:$LuVO_4$ crystals," Opt. Lett. **31**(22), 3294-3296 (2006).
23. A. Rudenkov, V. Kisel, A. Yasukevich, K. Hovhannesyan, A. Petrosyan, and N. Kuleshov, "Yb^{3+}:$LuAlO_3$ crystal as a gain medium for efficient broadband chirped pulse regenerative amplification," Opt. Lett. **42**(13), 2415-2418 (2017).
24. J. Liu, H. Zhang, J. Wang, and V. Petrov, "Continuous-wave and Q-switched laser operation of Yb:$NaY(WO_4)_2$ crystal," Opt. Express **15**(20), 12900-12904 (2007).
25. J. Liu, V. Petrov, X. Mateos, H. Zhang, and J. Wang, "Efficient high-power laser operation of Yb:$KLu(WO_4)_2$ crystals cut along the principal optical axes," Opt. Lett. **32**(14), 2016–2018 (2007).
26. X. Chen, L. Wang, J. Liu, Y. Guo, W. Han, H. Xu, H. Yu, and H. Zhang, "High-power CW and passively Q-switched laser operation of Yb:$GdCa_4O(BO_3)_3$ crystal," Opt. Laser Tehcnol. **79**, 74-78 (2016).
27.] J. Liu, X. Mateos, H. Zhang, J. Li, J. Wang, and V. Petrov, "High-power laser performance of Yb:$YAl_3(BO_3)_4$ crystals cut along the crystallographic axes," IEEE J. Quantum Electron. **43**(5), 385-390 (2007).
28. J. M. Serres, V. Jambunathan, P. Loiko, X. Mateos, H. Yu, H. Zhang, J. Liu, A. Lucianetti, T. Mocek, K. Yumashev, U. Griebner, V. Petrov, M. Aguiló, and F. Díaz, "Microchip laser operation of Yb-doped gallium garnets," Opt. Mater. Express **6**(1), 46-57 (2016).